J|A|C|S
ARTICLES
Published on Web 10/09/2007

Scaling Laws for Charge Transfer in Multiply Bridged Donor/Acceptor Molecules in a Dissipative Environment

Randall H. Goldsmith, Michael R. Wasielewski,* and Mark A. Ratner*

Contribution from the Department of Chemistry, Argonne-Northwestern Solar Energy Research (ANSER) Center, and International Institute for Nanotechnology, Northwestern University, Evanston, Illinois 60208-3113

Received May 18, 2007; E-mail: m-wasielewski@northwestern.edu; ratner@northwestern.edu

Abstract: The ability of multiple spatial pathways to sum coherently and facilitate charge transfer is examined theoretically. The role of multiple spatial pathways in mediating charge transfer has been invoked several times in the recent literature while discussing charge transfer in proteins, while multiple spatial pathways are known to contribute to charge transport in metal−molecule−metal junctions. We look at scaling laws for charge transfer in donor−bridge−acceptor (D−B−A) molecules and show that these scaling laws change significantly when environment-induced dephasing is included. In some cases, D−B−A systems are expected to show no enhancement in the rate of charge transfer with the addition of multiple degenerate pathways. The origins of these different scaling laws are investigated by looking at which Liouville space pathways are active in different dephasing regimes.

Introduction

The search for vectorial charge and excitation transfer in molecules and nanostructures is motivated by advances in the design of molecular electronic and photonic devices,[1] insights into the microscopic processes in photovoltaics,[2] and furthering our understanding of photosynthesis.[3] Studies in this last category have shown that multiple spatial pathways may contribute to the overall charge and exciton transfer rates.[4−7] The explanation of observed experimental rates advanced in some of these studies demands that coherences exist among different and not necessarily proximal spatial pathways. However, the nature of the environment surrounding these paths will determine whether those coherences can survive.[8,9] Consequently, rules governing the additivity of multiple spatial pathways for charge and exciton transfer, rules that include a dissipative environment, must be addressed. Beyond charge and exciton transfer in proteins, conductance measurements on self-assembled monolayers of molecules implicitly involve measurements on many molecules simultaneously, and any kind of extrapolation regarding the behavior of a single molecule must be made very carefully. Conductance measurements on molecules in mechanically produced break junctions often result in integer multiples of some unit of molecular conductance,[10] implying additive contributions from multiple molecules.

Several theoretical efforts have examined the additivity of multiple spatial molecular conduction channels. Lang and Avouris[11] and Yaliraki and Ratner[12] concentrated on "crosstalk" interactions between contributing molecules, while Larsson[13] and Magoga and Joachim[14] looked at scaling laws for transport through multiple equivalent spatial pathways. Magoga and Joachim predicted that as the number of spatially distinct pathways (N) increased, the conductance should increase either linearly or quadratically (with N), depending on the system connectivity. If the molecules were each individually connected to the leads, the linear law would apply, whereas if the molecules were connected by some molecular node before connecting to the lead, the quadratic law would apply. Several efforts in a number of different experimental test beds have demonstrated a linear dependence, although some deviations appeared with large N.[10,15,16]

All of these theoretical studies investigated the coherent limit. However, the environment is known to cause the system to lose coherence,[8,9] and previous studies have shown that interference can be significantly affected by a dissipative environment.[17−19] When applied to transport in donor−bridge−acceptor (D−B−

(1) Cuniberti, G.; Fagas, G.; Richter, K. *Introducing Molecular Electronics*; Springer Verlag: Berlin, 2005; Vol. 680.
(2) Sun, S.-S.; Sariciftci, N. S. *Organic Photovoltaics: Mechanisms, Materials, and Devices*; CRC Press: Boca Raton, FL, 2005.
(3) Wasielewski, M. R. *Chem. Rev.* **1992**, *92*, 435−461.
(4) Balabin, I. A.; Onuchic, J. N. *Science* **2000**, *290*, 114−117.
(5) Kawatsu, T.; Beratan, D. N.; Kakitani, T. *J. Phys. Chem. B* **2006**, *110*, 5747−5757.
(6) Kuki, A.; Wolynes, P. G. *Science* **1987**, *236*, 1647−1652.
(7) Prytkova, T. R.; Kurnikov, I. V.; Beratan, D. N. *Science* **2007**, *315*, 622−625.
(8) Skinner, J. L.; Hsu, D. *J. Phys. Chem.* **1986**, *90*, 4931−4938.
(9) Nitzan, A. *Annu. Rev. Phys. Chem.* **2001**, *52*, 681−750.
(10) Xiao, X. Y.; Xu, B. Q.; Tao, N. J. *Nano Lett.* **2004**, *4*, 267−271.
(11) Lang, N. D.; Avouris, P. *Phys. Rev. B* **2000**, *62*, 7325−7329.
(12) Yaliraki, S. N.; Ratner, M. A. *J. Chem. Phys.* **1998**, *109*, 5036−5043.
(13) Larsson, S. *J. Am. Chem. Soc.* **1981**, *103*, 4034−4040.
(14) Magoga, M.; Joachim, C. *Phys. Rev. B* **1999**, *59*, 16011−16021.
(15) Blum, A. S.; Kushmerick, J. G.; Pollack, S. K.; Yang, J. C.; Moore, M.; Naciri, J.; Shashidhar, R.; Ratna, B. R. *J. Phys. Chem. B* **2004**, *108*, 18124−18128.
(16) Kushmerick, J. G.; Naciri, J.; Yang, J. C.; Shashidhar, R. *Nano Lett.* **2003**, *3*, 897−900.
(17) Caldeira, A. O.; Leggett, A. J. *Phys. Rev. A* **1985**, *31*, 1059−1066.
(18) Goldsmith, R. H.; Wasielewski, M. R.; Ratner, M. A. *J. Phys. Chem. B* **2006**, *110*, 20258−20262.
(19) Skourtis, S. S.; Waldeck, D. H.; Beratan, D. N. *J. Phys. Chem. B* **2004**, *108*, 15511−15518.

 10.1021/ja073589b CCC: $37.00

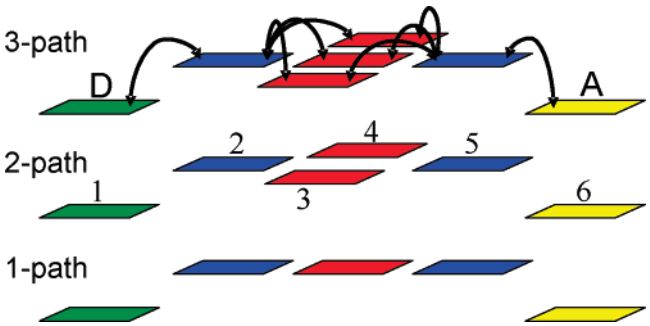

Figure 1. Connectivities of multiple spatial pathway donor−bridge−acceptor systems. The red (bridge) and blue (node) sites are energetically degenerate. The numbers denote the sites.

A) molecules, the inclusion of dephasing enables the operation of a new and qualitatively different transport regime: the incoherent or hopping transport mechanism. Calculations predicted different length dependencies for the purely coherent superexchange mechanism and the incoherent mechanism,[20−23] predictions that were later borne out experimentally.[24−27] The aim of this report is to make similar predictions about the dependence on N of superexchange and incoherent transport, and to explore more generally how decoherence affects the role of multiple spatial pathways in charge transfer in D−B−A molecules.

Method

Our calculation utilizes a simple and purely electronic[28] tight-binding Hamiltonian which completely defines the system connectivity. D and A sites are taken to be degenerate and define the zero energy level of the system. All bridge sites are taken to be ω above the D and A sites in energy. All couplings are of magnitude V. Following the approach of Bixon and Jortner, an absorbing boundary condition (an energy width of magnitude κ, with $\kappa \sim 1/T_1$) simulates the final deposition of a charge carrier within the vibrational manifold of the A site, causing irreversible, as opposed to oscillatory, charge transfer.[29]

Equations of motion (EOM) are expressed using the density matrix formalism with dynamics determined by the quantum-Liouville equation.

$$\dot{\rho} = \frac{-i}{\hbar}[H,\rho] + L_{\mathrm{D}}\rho \qquad (1)$$

Solution of the dynamics constitutes an initial value problem (IVP), with the initial condition simply being all carrier population beginning on the D site (representing photoexcitation). The IVP can be solved, albeit with some difficulty, via spectral decomposition. An alternate method of solution entails forcing the system to reach a non-trivial steady state (SS), followed by relating the flux through the system at this SS to the rate from the IVP.[30] More specifically, the terms describing the dynamics of the D site are modified so that the population remains constant. This constant population keeps the system from reaching a trivial SS by replenishing population lost via the absorbing boundary condition. There are two ways of executing this modification: [22] one method (termed "constant population") involves modifying only the EOM of the diagonal elements of the density matrix (ρ), while the other (termed "constant amplitude and phase") also involves modification of the EOM of the coherences associated with the D site. We want to emphasize that our use of this forced SS method is to simplify solving our IVP, and so the latter method is chosen because of better agreement with the solution of the IVP. Conditions for agreement between the SS and IVP methods have been addressed previously[23] and will be further discussed below. Related approaches have been used previously to look at charge-transfer rates in D−B−A systems,[20,22,23] most recently in multiple spatial pathway systems[18] and dendrimers.[31] All EOM are given in the Supporting Information.

Pure dephasing is added to the calculation by modulation of the EOM for the coherences in the density matrix linking the various sites. We use the term "pure dephasing" to include any elastic process that destroys phase relationships within the wave function of the charge carrier as it passes through the sites of the system without directly affecting the populations.[9,32] When applied to an ensemble of molecules, signals that rely on a coherent sum from members of the ensemble decay, often exponentially, with some characteristic time constant, called T_2 in magnetic resonance literature. However, the concept can also be applied to just a single member of an ensemble, where the density matrix, instead of providing statistical information about the ensemble, reflects uncertainty in our knowledge about the state. We include pure dephasing by adding to the EOM for the coherences $\rho_{ij,i\neq j}$, a decay term first order in ρ_{ij} with rate constant γ, where essentially $\gamma = 1/T_2^*$. It is then apparent that dephasing over time converts the pure state (with maximum coherence $\rho_{ij} = |\rho_{ii}\rho_{jj}|^{1/2}$) to a statistical mixture of diabatic states (with vanishing coherence). This form of dephasing, affecting only the off-diagonal elements of ρ, arises from fluctuations in the energy levels of the diabatic states and is caused by shifts in the diagonal elements of the Hamiltonian. Skinner and Hsu have derived the first-order rate process form of pure dephasing using both quantum mechanical and stochastic formulations.[8] For a D−B−A molecule in solution, vibrational interaction with the solution bath and intramolecular vibrations will likely be the dominant contributions. Ignoring small fluctuations in the off-diagonal elements of the Hamiltonian is valid in the weak electronic coupling regime.[33] The value of γ ($1/T_2^*$) and its temperature dependence will depend on vibrational coupling[8] as well as the spectral density of the bath.[33,34] Assumption of a Markovian bath with vanishing correlation time yields the familiar Redfield picture.[35] EOM of the off-diagonal elements of ρ have contributions from both pure dephasing and relaxation, consistent with the Bloch relation,

$$\frac{1}{T_2} = \frac{1}{T_2^*} + \frac{1}{2T_1} \qquad (2)$$

In our model, the diabatic states are part of an electronic site basis. Consequently, dephasing results in a loss of the wave function's ability to spread over multiple sites, and localization ensues. Pure electronic dephasing rates of chromophores have been reported over a range of values, with coherence lifetimes $T_2^* \gg 10$ ps ($\gamma \ll 3$ cm^{-1}) at liquid helium temperatures and $T_2^* < 0.1$ ps ($\gamma > 300$ cm^{-1}) projected for

(20) Davis, W. B.; Wasielewski, M. R.; Ratner, M. A.; Mujica, V.; Nitzan, A. *J. Phys. Chem. A* **1997**, *101*, 6158−6164.
(21) Felts, A. K.; Pollard, W. T.; Friesner, R. A. *J. Phys. Chem.* **1995**, *99*, 2929−2940.
(22) Segal, D.; Nitzan, A. *Chem. Phys.* **2001**, *268*, 315−335.
(23) Segal, D.; Nitzan, A.; Davis, W. B.; Wasielewski, M. R.; Ratner, M. A. *J. Phys. Chem. B* **2000**, *104*, 3817−3829.
(24) Davis, W. B.; Svec, W. A.; Ratner, M. A.; Wasielewski, M. R. *Nature* **1998**, *396*, 60−63.
(25) Goldsmith, R. H.; Sinks, L. E.; Kelley, R. F.; Betzen, L. J.; Liu, W. H.; Weiss, E. A.; Ratner, M. A.; Wasielewski, M. R. *Proc. Natl. Acad. Sci. U.S.A.* **2005**, *102*, 3540−3545.
(26) Weiss, E. A.; Ahrens, M. J.; Sinks, L. E.; Gusev, A. V.; Ratner, M. A.; Wasielewski, M. R. *J. Am. Chem. Soc.* **2004**, *126*, 5577−5584.
(27) Xu, B. Q.; Zhang, P. M.; Li, X. L.; Tao, N. J. *Nano Lett.* **2004**, *4*, 1105−1108.
(28) Ratner, M. A.; Ondrechen, M. J. *Mol. Phys.* **1976**, *32*, 1233−1245.
(29) Bixon, M.; Jortner, J. *Adv. Chem. Phys.* **1999**, *106*, 35−202.
(30) Nitzan, A. *Chemical Dynamics in Condensed Phases: Relaxation, Transfer, and Reactions in Condensed Molecular Systems*; Oxford University Press: New York, 2006.
(31) Kalyanaraman, C.; Evans, D. G. *Nano Lett.* **2002**, *2*, 437−441.
(32) Onuchic, J. N.; Wolynes, P. G. *J. Phys. Chem.* **1988**, *92*, 6495−6503.
(33) Leggett, A. J.; Chakravarty, S.; Dorsey, A. T.; Fisher, M. P. A.; Garg, A.; Zwerger, W. *Rev. Mod. Phys.* **1987**, *59*, 1−85.
(34) Reichman, D.; Silbey, R. J.; Suarez, A. *J. Chem. Phys.* **1996**, *105*, 10500−10506.
(35) Redfield, A. G. *IBM J. Res. Dev.* **1957**, *1*, 19−31.

chromophores in solution at room temperature.[36] The rates are measured using spectral hole burning, photon echo, or resonance Raman techniques among others.[37] More recently, two-color photon echo techniques have explored the dephasing time between non-degenerate chromophores and even suggested that a protein sheath might play a role in preserving coherences.[38,39] The many solution studies of chromophores show electronic dephasing times loosely clustered in the range given above,[37] suggesting these are good values for a "typical" chromophore, although future two-color experiments are necessary and should show the inter-chromophore dephasing rate to be sensitive to the vibronic coupling between chromophores and solvent and the solvent's vibrational spectral density.[36,37,40−42] The lifetime of the coherence between a fully occupied state and a weakly occupied state (although not yet a virtual state, which would have no dephasing based on Büttiker−Landauer tunneling time arguments[43]) is a more subtle issue and is currently under theoretical investigation. Rational modulation of the electronic dephasing time could possibly be effected by altering the magnitude of solvent-induced energetic fluctuations and correlation times, which could be accomplished by varying solvent dipole moment, viscosity, and temperature.

The concept of a participation ratio (PR) has been introduced[44] to give a measure of the delocalization of the wave function and recently applied[45,46] in the context of electron transfer. Mukamel and co-workers[47,48] have adapted the PR concept for the density matrix and used it as a measure of the coherence length. They define two quantities, the population participation ratio (PPR),

$$\mathrm{PPR} = \left(\sum_n \rho_{nn}{}^2\right)^{-1} \tag{3}$$

and the coherence participation ratio (CPR),

$$\mathrm{CPR} = \frac{\left(\sum_{mn} |\rho_{mn}|\right)^2}{\mathrm{PPR} \sum_{mn} |\rho_{mn}|^2} \tag{4}$$

The PPR ranges from 1 to N and gives a measure of the number of sites at which the charge carrier is likely to be found. The CPR reflects the strength of the phase relationships between those sites and is indicative of delocalization.

Results

We begin by examining the system geometries shown in Figure 1, in the coherent limit. In the highly non-resonant regime, with $\omega \gg V,\kappa$ (variables defined in the above text), we determined the analytical solutions for the rate constant of ET to take the form

$$k_{\mathrm{ET}} = \frac{4N^2 V^2}{\kappa}\left(\frac{V}{\omega}\right)^{2L} \tag{5}$$

where the charge-transfer rate constant is seen to vary as the square of the number of pathways (N). The rate expression's dependence on L, the number of linear bridge units, has been discussed previously.[20]

Magoga and Joachim[14] have predicted this quadratic dependence (on N) for systems that converge to single molecular nodes before coupling to the band structure of an electrode.

The calculated ratio of the rates for the N-pathway system to the single-pathway system is plotted in Figure 2. The value of ω, the B energy gap, of 8000 cm^{-1} (1 eV) is consistent with a small aromatic bridge, while the V coupling between sites, 500 cm^{-1}, corresponds to a typical coupling between individual phenyl rings. The decay rate from the A site, κ, is set at 400 cm^{-1}, following previous investigations.[23] The small deviations from the N^2 limit on the left-hand side of the plots are indicative of the relatively weak but finite dephasing as well as not being completely in the highly non-resonant regime. The absolute rate for the linear system ($N = 1$) is shown for comparison.

Dephasing is initially added to the EOM for all of the coherences involving B (red and blue) sites (Figure 2A). As the dephasing rate is increased, the rate ratios for the multiple pathway structures decrease and ultimately converge to unity. In contrast, the absolute rate of the linear system increases with γ (until $\gamma \approx \omega$), as shown previously.[20] Pure dephasing opens up an additional incoherent transport channel that quickly overwhelms the superexchange channel. This incoherent channel is seen to be independent of N, the number of pathways. Just as the shift from superexchange to incoherent transport results in a different length dependence for ET, this same shift also results in a different dependence on the number of spatial pathways.

Modulation of the system parameters leaves Figure 2 qualitatively unchanged. Decreasing ω makes the rate ratio less sensitive to γ. This is consistent with earlier work,[20] as a smaller energetic barrier enhances the contribution of the coherent channel to a greater extent than it enhances the incoherent channel, allowing the coherent limit of the rate ratio to survive over a larger range of dephasing strengths. Modulation of V distorts the shape of the rate ratio curve, but the coherent and incoherent ratio limits are preserved, as long as the system remains in the highly non-resonant regime. Changing κ has minimal effect, as long as κ remains small compared to ω.

To verify that the SS method returns the correct solution to the IVP, we also solved the IVP directly for several values of γ. These values are also seen in the rate ratio plots (for $N = 1$) and show good agreement with the SS method. At higher values of γ, the IVP rates become multiexponential and the rate calculated by the SS method may become irrelevant. As discussed by Segal, Nitzan, and co-workers,[23] the conditions for the system attaining a monoexponential decay (and thus agreeing with the SS method) entail the system reaching a pre-equilibrium very quickly compared to the total population decay. If the system can attain this pre-equilibrium fast enough, the multisite system behaves essentially as a single carrier reservoir and obeys first-order kinetics. This situation is similar to SS approximation behavior in simple classical chemical kinetics.

(36) Toutounji, M.; Small, G. J.; Mukamel, S. *J. Chem. Phys.* **1999**, *110*, 1017−1024.
(37) Myers, A. B. *Annu. Rev. Phys. Chem.* **1998**, *49*, 267−295.
(38) Lee, H.; Cheng, Y. C.; Fleming, G. R. *Science* **2007**, *316*, 1462−1465.
(39) Sension, R. J. *Nature* **2007**, *446*, 740−741.
(40) Jackson, B.; Silbey, R. *Chem. Phys. Lett.* **1983**, *99*, 331−334.
(41) Reinot, T.; Kim, W. H.; Hayes, J. M.; Small, G. J. *J. Chem. Phys.* **1997**, *106*, 6205−6205.
(42) Vohringer, P.; Arnett, D. C.; Westervelt, R. A.; Feldstein, M. J.; Scherer, N. F. *J. Chem. Phys.* **1995**, *102*, 4027−4036.
(43) Nitzan, A.; Jortner, J.; Wilkie, J.; Burin, A. L.; Ratner, M. A. *J. Phys. Chem. B* **2000**, *104*, 5661−5665.
(44) Bell, R. J.; Dean, P. *Discuss. Faraday Soc.* **1970**, *50*, 55−61.
(45) Elicker, T. S.; Evans, D. G. *J. Phys. Chem. A* **1999**, *103*, 9423−9431.
(46) Evensky, D. A.; Scalettar, R. T.; Wolynes, P. G. *J. Phys. Chem.* **1990**, *94*, 1149−1154.
(47) Meier, T.; Zhao, Y.; Chernyak, V.; Mukamel, S. *J. Chem. Phys.* **1997**, *107*, 3876−3893.
(48) Kirkwood, J. C.; Scheurer, C.; Chernyak, V.; Mukamel, S. *J. Chem. Phys.* **2001**, *114*, 2419−2429.

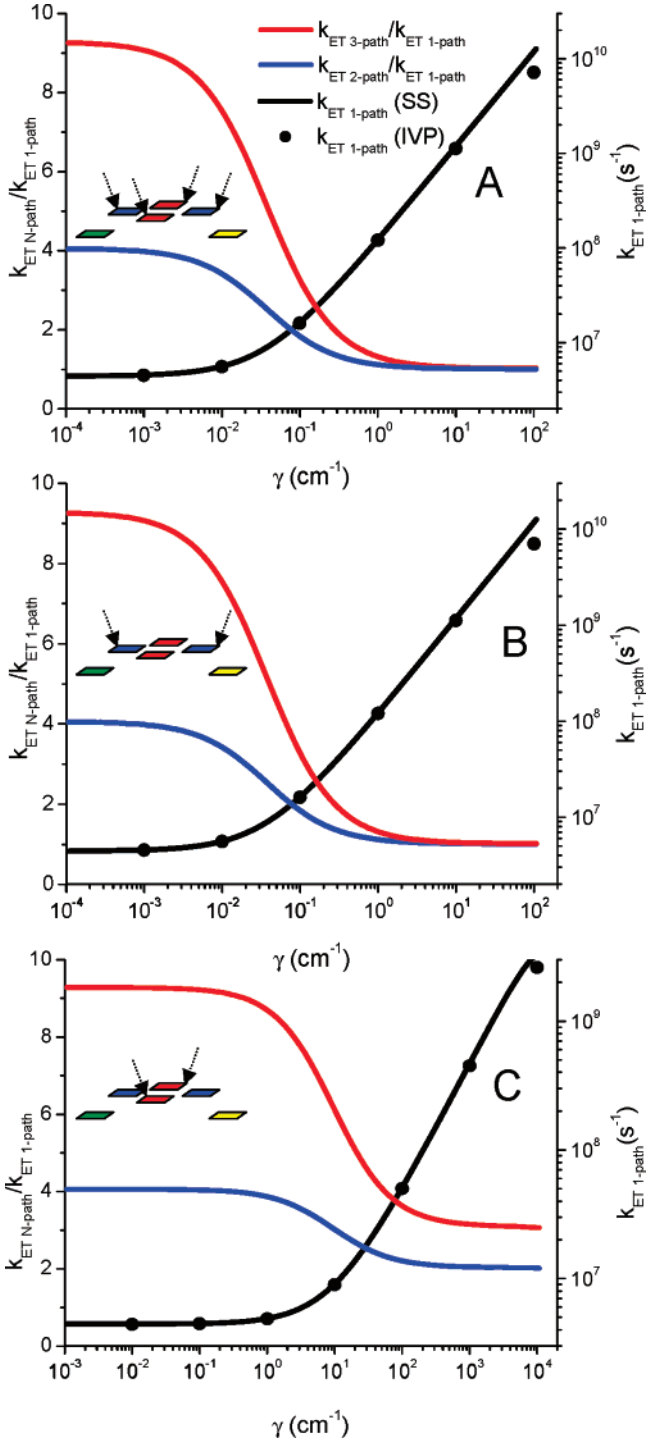

Figure 2. Rate ratios for the two- (blue line) and three-path (red line) systems, absolute rate for the one-path system (black line) calculated with the enforced SS, and comparison with that rate calculated as an IVP (black circle). These values were calculated for increasing dephasing on the red and blue sites (A), just the blue sites (B), and just the red sites (C).

Previous studies of the influence of pure dephasing on ET have shown that the representation[13,49,50] in which dephasing is introduced can significantly influence the transport behavior. In the limit of extremely fast decoherence, these different representations correspond to different environment-induced superselection (einselection) operations, resulting in different

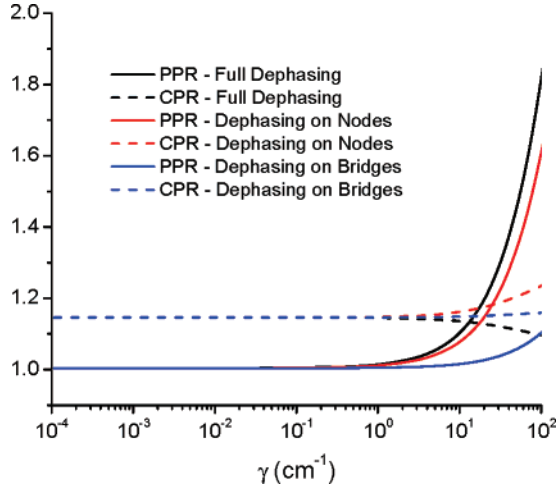

Figure 3. Participation ratios with different dephasing schemes.

"pointer states" being available for measurement.[51] Consequently, we varied the dephasing behavior within the site basis, dephasing on just the nodes (the blue sites in Figure 1), as shown in Figure 2B, and dephasing on just the degenerate bridge sites (the red sites in Figure 1), as shown in Figure 2C. The effect of dephasing on the nodes is nearly identical to that of dephasing on all of the B sites. However, dephasing only on the degenerate bridge sites yields qualitatively different behavior. Instead of converging to unity, the rate ratios converge to N. Magoga and Joachim[14] predicted a linear dependence on N for molecular junctions where multiple molecular pathways connected with the electrode without connecting first via a molecular node, while a linear dependence was also observed in several experimental junctions whose geometry has this character.[15,16] This different dephasing scheme also more weakly hinders the formation of the pre-equilibrium as compared to the other two dephasing schemes. Consequently, it is possible to examine rate ratios at much higher values of γ, although values much greater than 10^2 cm^{-1} are likely unphysically large.

Discussion

To better understand this shift from quadratic to linear dependence, we looked more closely at the pre-equilibrium. As stated before, the formation of this pre-equilibrium is necessary for the validity of the SS approximation. However, the nature of this pre-equilibrium, and the values of the populations and coherences, may help us understand, mechanistically, the action of the different dephasing schemes.

In Figure 3, we plot the PPR and CPR with increasing dephasing strength for the different dephasing schemes for the $N = 2$ system. The PPR (solid lines) correctly captures the gradual shift to more population existing on the B sites at higher values of γ, although most of the population still resides on the D site. When dephasing operates only on the degenerate bridge sites (as in Figure 2C), less population accumulates on the B sites than other dephasing schemes at equivalent γ. Maintaining population mainly on the D site is a necessary condition for agreement between the SS and IVP methods.[23]

Unfortunately, the CPR shows very little change. Because the value of the CPR is dominated by the stronger coherence values, it cannot give us information about potentially important

(49) Volkovich, R.; Peskin, U. *J. Chem. Phys.* **2006**, *125*, 244505.
(50) Weiss, E. A.; Katz, G.; Goldsmith, R. H.; Wasielewski, M. R.; Ratner, M. A.; Kosloff, R.; Nitzan, A. *J. Chem. Phys.* **2006**, *124*, 1−6.
(51) Ollivier, H.; Poulin, D.; Zurek, W. H. *Phys. Rev. A* **2005**, *72*, 42113.

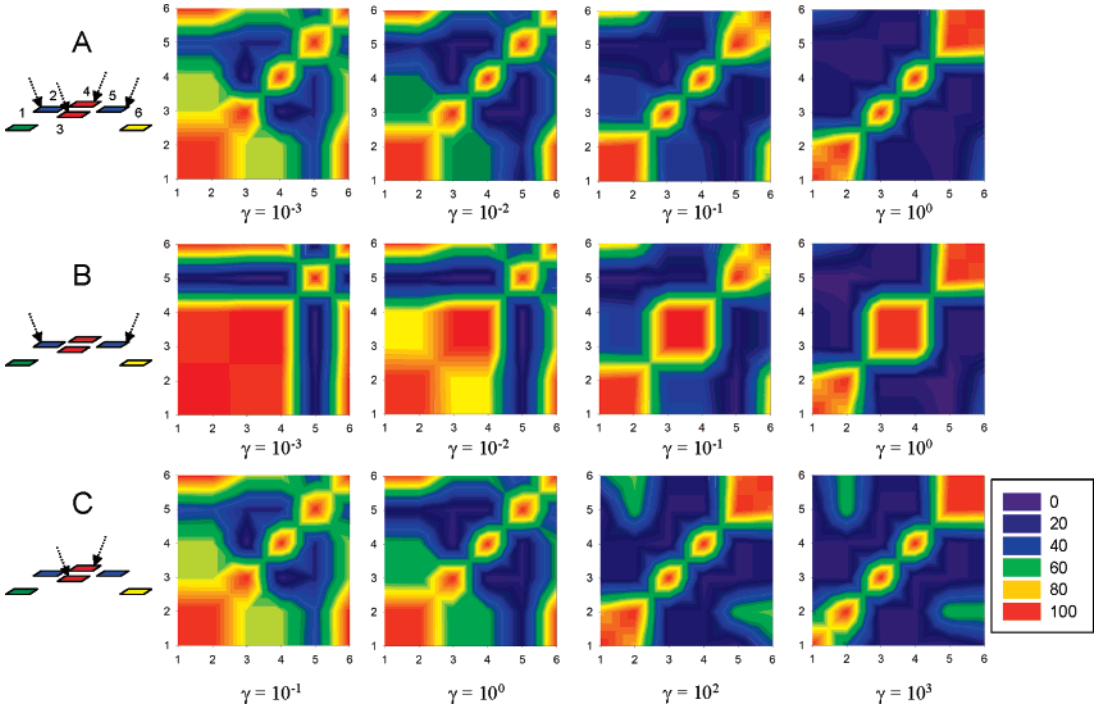

Figure 4. Plots of the percent maximal coherence (PMC) of each position of the density matrix at increasing dephasing strengths for three dephasing schemes: dephasing on the red and blue sites (A), the blue sites (B), and the red sites (C). The numbers on the axes denote the different sites (from Figure 1).

changes in the weaker coherences. To examine these changes, we adopt a strategy related to Mukamel and co-workers' real-space plotting of the density matrix.[52] Rather than showing the absolute values of the coherences, where even with a logarithmic scale small changes in the weaker coherences would be difficult to see, we plot a quantity we term the percent maximum coherence (PMC), which we define as

$$\mathrm{PMC}_{ij} = \frac{\rho_{ij}}{\sqrt{|\rho_{ii}\,\rho_{jj}|}} \times 100 \qquad (6)$$

In a pure state (i.e., ρ is idempotent), the PMC will be 100, while in a statistical mixture of states, the PMC is 0. Notice that, by definition, diagonal elements of the density matrix have a PMC of 100. In Figure 4, PMCs are plotted for the pre-equilibria formed for different dephasing schemes at selected dephasing strengths.

The PMC plots can provide information as to which Liouville space pathways[53] offer the greatest contributions for transport. Positioning the decoherences on the nodes (Figure 4B) compared to the full dephasing (Figure 4A) treatment shows PMC plots that differ only in the coherences between degenerate bridge sites. However, since these two decoherence schemes show only marginal effect on the rate ratio, these coherences likely constitute an irrelevant Liouville space pathway, as is physically reasonable.

An interesting issue is the distinction between the scenario where the newly opened incoherent channel simply dominates the transport and the scenario where the dephasing actually reduces the absolute effectiveness of the coherent, superexchange channel. One definition of superexchange defines the process as requiring passage through the ρ_{DA} or ρ_{AD} Liouville state.[53] At values of $\gamma > 10^{-3}$, the incoherent channel quickly becomes dominant (as evidenced by the increased absolute rate), while only at values of $\gamma > 10^{-1}$ does the PMC of ρ_{DA} decrease in magnitude. This implies a reduction in the efficacy of superexchange at high γ, showing that both scenarios are correct: the incoherent channel quickly overshadows the coherent channel, which, already reduced in relative contribution, eventually becomes reduced in absolute contribution.

The coherence ρ_{DA} retains its high PMC over a much larger γ with dephasing applied only on the degenerate bridges. In our calculations on linear systems, we found that the impact of dephasing on a particular site was significantly enhanced by that site's proximity to the starting point of the carrier. While other explanations for dephasing contact effects have been suggested,[49] we feel that this condition is likely causing the weaker effects in this dephasing scheme. However, the origin of the different convergent rate ratio (Figure 2A,B as compared to C) needs to be addressed. In all parts of Figure 4, the PMC of ρ_{DA} significantly diminishes at large dephasing strengths. On the other hand, the PMC of ρ_{25} (the coherence between the nodes, red sites, see Figure 1) retains a relatively large value even into unphysically large dephasing ranges for Figure 4C. The absence of this Liouville path in the other decoherence schemes, as evidenced by the lack of PMC at that position, implies that this path is responsible for the different convergent rate ratio. This behavior makes sense when one looks at the subsystem made up of just the red and blue sites (a valid perspective since the coherence ρ_{DA} has already become negligible). All of the sites in this subsystem are energetically degenerate, and the coherences between the red sites have been destroyed (PMC = 0). Without these interference terms to cause the N^2 dependence, the two pathways will sum like classical microscopic rate processes, with $k_{tot} = Nk_{micro}$.

(52) Mukamel, S.; Tretiak, S.; Wagersreiter, T.; Chernyak, V. *Science* **1997**, *277*, 781−787.
(53) Skourtis, S. S.; Mukamel, S. *Chem. Phys.* **1995**, *197*, 367−388.

As mentioned above, this situation is qualitatively similar to the one discussed by Magoga and Joachim regarding the N dependence of the conductance of molecules individually wired to the electrodes. In that case also, the interference terms are destroyed, resulting in the N dependence. However, in their work it is the band structure of the electrodes that causes the critical coherences to be destroyed, while in this case, it is the environment that causes those terms' destruction.

In the coherent limit (no dephasing), the Liouville pathway connecting the D and A sites is dominant, and the contributions from the multiple spatial pathways sum coherently to give the N^2 dependence, as is expected for superexchange. When we dephase on the nodes, all relevant coherences are destroyed and incoherent transport dominates. In this situation, the localized charge carrier must essentially choose a single pathway, regardless of the number of pathways available, leading to the rate ratio of unity.

Conclusion

In summary, we have examined charge-transfer model systems representing D−B−A molecules with multiple spatial pathways, using a combination of enforced SS and IVP methods. After returning rate ratios that are in agreement with what others have predicted in the coherent limit, we have shown that adding pure (or T_2*) dephasing significantly affects the rate ratio. In addition, we observed different convergent rate ratios, depending on which local decoherence scheme was applied. We examined the differences between these schemes by looking at the percent maximum coherence of the different elements of the corresponding density matrix of the pre-equilibrium attained. Different decoherence schemes opened up different Liouville pathways that are responsible for the respective rate ratios. These pathways show rate ratios that vary from an N^2 dependence for full coherence, to an N dependence for dephasing only on the parallel bridge sites, to no dependence on N for dephasing on the nodes.

Acknowledgment. We thank Professors Abraham Nitzan and Vladimiro Mujica, as well as Eric Greyson, Joshua Vura-Weis, and Zachary Dance, for very helpful conversations. R.H.G. thanks the Link Foundation and the Dan David Foundation for fellowships. This research was supported by the Chemical Sciences, Geosciences, and Biosciences Division, Office of Basic Energy Sciences, U.S. Department of Energy, under grant no. DE-FG02-99ER14999 (M.R.W.). M.A.R. thanks the Chemistry Division of the NSF, the Northwestern MRSEC, and the ONR for support.

Supporting Information Available: Full equations of motion. This material is available free of charge via the Internet at http://pubs.acs.org.

JA073589B